Perturbative Linearization of Reaction-Diffusion Equations

Sanjay Puri[1] and Kay Jörg Wiese[2]

[1]School of Physical Sciences, Jawaharlal Nehru University, New Delhi – 110067, India.

[2] KITP, Kohn Hall, University of California at Santa Barbara, Santa Barbara, CA, 93106-4030, U.S.A.

February 1, 2008

Abstract

We develop perturbative expansions to obtain solutions for the initial-value problems of two important reaction-diffusion systems, viz., the Fisher equation and the time-dependent Ginzburg-Landau (TDGL) equation. The starting point of our expansion is the corresponding singular-perturbation solution. This approach transforms the solution of nonlinear reaction-diffusion equations into the solution of a hierarchy of linear equations. Our numerical results demonstrate that this hierarchy rapidly converges to the exact solution.

1   Introduction

Many physical problems are described by nonlinear partial differential equations (pdes). In particular, much research interest has focused upon two classes of nonlinear pdes, viz.,

(i) *soliton-bearing equations*, which arise in the context of completely-integrable infinite-dimensional Hamiltonian systems [1,2]; and

(ii) *reaction-diffusion equations*, which arise in the context of pattern-forming systems where local reactions are combined with spatial diffusion [3–6].

There is no general framework for obtaining the solution of the initial-value problem for an arbitrary nonlinear pde. For the class of soliton-bearing equations in (i), powerful techniques like the *inverse scattering transform* and *Backlund transformations* enable the solution of these equations for arbitrary initial conditions [1,2]. Essentially, these methods reduce the problem of solution of a nonlinear soliton equation to a sequence of linear equations. In a related context, a classic example of linearization is provided by the Cole-Hopf transformation [7], which transforms the nonlinear Burgers' equation [8] into the linear diffusion equation.

For the class of reaction-diffusion equations in (ii) above, there are as yet no systematic methods of linearization. These pdes have the general form:

$$\partial_t \psi(\vec{r}, t) = f(\psi) + \nabla^2 \psi, \tag{1.1}$$

where $\psi(\vec{r}, t)$ is an order-parameter field, e.g., population density, chemical concentration, magnetization, which depends on space ($\vec{r}$) and time (t). The order parameter may be either scalar or vector, depending upon the number of variables which describe the physical system. The order parameter evolves in time due to a local reaction, described by the nonlinear term $f(\psi)$, in conjunction with spatial diffusion. Reaction-diffusion equations are ubiquitous in pattern-forming systems, ranging from chemical and biological physics to materials science and metallurgy [3–6].

An important example of Eq. (1.1) is the Fisher equation with $f(\psi) = \psi - \psi^2$, which describes the growth and saturation of a species population [9,10]. Another important reaction-diffusion model is the

time-dependent Ginzburg-Landau (TDGL) equation with $f(\vec{\psi}) = \vec{\psi} - |\vec{\psi}|^2\vec{\psi}$ [11,12], where $\vec{\psi}$ is an n-component vector, $\vec{\psi} \equiv (\psi_1, \psi_2, ..., \psi_n)$. The case with $n = 1$ describes the phase ordering dynamics of a ferromagnet which has been suddenly quenched from the paramagnetic phase to the ferromagnetic phase. The TDGL equation with $n = 2$ describes phase ordering dynamics in superconductors, superfluids and liquid crystals [12]. In this paper, we will investigate the perturbative linearization of the Fisher and TDGL equations for arbitrary initial conditions.

This paper is organized as follows. Section 2 provides an overview of relevant analytical results, primarily in the context of the Fisher equation. Section 3 discusses our linearization scheme and presents detailed numerical results therefrom. Finally, Section 4 concludes this paper with a summary and discussion of our results.

2 Overview of Analytical Results

Let us first consider the Fisher equation in an infinite domain, which has the following form [9]:

$$\partial_t \psi(\vec{r}, t) = \psi - \psi^2 + \nabla^2 \psi. \tag{2.1}$$

In general, Eq. (2.1) is supplemented with some arbitrary initial condition $\psi(\vec{r}, 0)$. Typically, we are interested in the case with $\psi \geq 0$, as the order parameter describes population density which cannot be negative. As a matter of fact, Eq. (2.1) is unstable for $\psi < 0$. The homogeneous solution $\psi^* = 0$ is an unstable fixed point (FP) of the dynamics. Fluctuations about $\psi^* = 0$ diverge exponentially and saturate to the stable FP, $\psi^* = 1$.

There is no general solution available for the initial-value problem of Eq. (2.1). However, some important analytical results are known for the case with dimensionality $d = 1$. Kolmogorov *et al.* [10] found that the Fisher equation has stable traveling-wave solutions $\psi(x, t) \equiv \psi(x - vt)$ (called *clines*), which are domain walls with
(a) velocity $v \geq 2$, and $\psi(-\infty, t) = 1$, $\psi(\infty, t) = 0$; or
(b) velocity $v \leq -2$, and $\psi(-\infty, t) = 0$, $\psi(\infty, t) = 1$.
The qualitative forms of these solutions are easily obtained through a phase-portrait analysis, but the explicit analytic forms are unknown.

In more general work, Aronson and Weinberger [13] considered the $d = 1$ version of Eq. (1.1). They focused on functions $f(\psi)$ which satisfy the conditions

$$\begin{aligned}
f(\psi) &\geq 0 \quad \text{for} \quad \psi \in [0, 1], \\
f(0) &= f(1) = 0, \\
f'(0) &> 0 > f'(1).
\end{aligned} \tag{2.2}$$

These authors demonstrated that a broad class of initial conditions $\psi(x, 0)$, with sharp interfaces, converge to a traveling-wave solution with a definite speed c^*, which satisfies

$$\begin{aligned}
2[f'(0)]^{1/2} &\leq c^* \leq 2L^{1/2}, \\
L = \sup \left[\frac{f(\psi)}{\psi} \right], &\quad \psi \in [0, 1].
\end{aligned} \tag{2.3}$$

A physical explanation of this velocity-selection principle has been formulated by various authors [14], and is often referred to as the *marginal stability hypothesis*. However, this approach has proven inadequate in

various applications. A more comprehensive understanding, based on structural-stability arguments, is due to Paquette *et al.* [15].

In the case of the Fisher equation, the Aronson-Weinberger result demonstrates that a large class of initial conditions converge to the cline solution with $v = \pm 2$, whose functional form is unknown as yet. An analytic form for a cline solution was first obtained by Ablowitz and Zeppetella [16] for $v = 5/\sqrt{6} > 2$.

It is of obvious interest to obtain analytic forms for other cline solutions, particularly the case $v = \pm 2$. It is of even greater interest to obtain a general solution for the initial-value problem of Eq. (2.1). In this context, Puri *et al.* [17] have used singular-perturbation techniques, developed by Suzuki [18] and Kawasaki *et al.* (KYG) [19] in the context of the TDGL equation, to obtain an approximate solution for the initial-value problem of the Fisher equation:

$$\tilde{\psi}_0(\vec{r}, t) = \frac{\psi_L(\vec{r}, t)}{1 + \psi_L(\vec{r}, t)},$$
$$\psi_L(\vec{r}, t) = e^{t(1+\nabla^2)} \psi(\vec{r}, 0), \tag{2.4}$$

where $\psi_L(\vec{r}, t)$ is the solution of the linear part of the Fisher equation, and diverges with time.

The approximate solution in Eq. (2.4) has a number of attractive features. For example, it is obtained for arbitrary dimensionality. Furthermore, initial conditions with sharp interfaces evolve into a traveling-wave front with asymptotic speed $v = 2$, in accordance with the Aronson-Weinberger result. The approach to the asymptotic velocity is as follows [17]:

$$v(t) \simeq 2 - \frac{d}{2t}. \tag{2.5}$$

Unfortunately, this is not in agreement with the exact result for the $d = 1$ Fisher equation obtained by Bramson [20]:

$$v(t) \simeq 2 - \frac{3}{2t}. \tag{2.6}$$

More generally, the fronts obtained using the singular-perturbation approximation are appreciably sharper than the exact result (obtained numerically) [17]. Furthermore, the solution in Eq. (2.4) is unable to accurately resolve front-front interactions [17]. An improved approximation has been proposed by Puri and Bray [21]. However, this is only valid for the less interesting class of initial conditions where the order parameter $\psi > 0$ everywhere, i.e., the evolving system is not characterized by the formation and interaction of fronts.

Finally, it is also relevant to discuss the singular-perturbation solution for the TDGL equation:

$$\partial_t \psi(\vec{r}, t) = \psi - \psi^3 + \nabla^2 \psi. \tag{2.7}$$

As mentioned earlier, the corresponding solution was obtained by KYG [19], who generalized a diagrammatic technique developed by Suzuki [18]. The approximate solution for the scalar TDGL equation is as follows:

$$\tilde{\psi}_0(\vec{r}, t) = \frac{\psi_L(\vec{r}, t)}{\sqrt{1 + \psi_L(\vec{r}, t)^2}},$$
$$\psi_L(\vec{r}, t) = e^{t(1+\nabla^2)} \psi(\vec{r}, 0). \tag{2.8}$$

Puri and Roland [22] have obtained the singular-perturbation solution for the 2-component TDGL equation. This result has been generalized by Bray and Puri [23] and Puri [24] to obtain the time-dependent structure

factor for the n-component TDGL equation. As in the case of the Fisher equation, the approximate solution in Eq. (2.8) is characterized by fronts which are too sharp. Furthermore, the singular-perturbation solution is unable to properly resolve domain-wall interactions [17].

In this paper, we undertake a perturbative improvement of the singular-perturbation solution of the Fisher and TDGL equations. We develop a hierarchy of linear equations which rapidly converges to the exact solution. Our primary goal is methodological, viz., demonstrating the equivalence between nonlinear reaction-diffusion equations and a sequence of linear equations.

3   Analytical and Numerical Results

3.1   Fisher Equation

The solution of the Fisher-equation with constant initial conditions suggests the following nonlinear transformation:

$$\psi(\vec{r}, t) = \frac{\phi(\vec{r}, t)}{1 + \phi(\vec{r}, t)}, \tag{3.1}$$

where $\phi > 0$ is an auxiliary field [12]. We confine ourselves to the physically interesting case with $1 > \psi \geq 0$. The corresponding pde satisfied by $\phi(\vec{r}, t)$ is

$$\partial_t \phi(\vec{r}, t) = \phi + \nabla^2 \phi - \frac{2(\nabla\phi)^2}{1 + \phi},$$

$$\phi(\vec{r}, 0) = \frac{\psi(\vec{r}, 0)}{1 - \psi(\vec{r}, 0)}. \tag{3.2}$$

The singular-perturbation approximation is equivalent to dropping the nonlinear term on the right-hand-side (RHS) of Eq. (3.2). In that case, the solution (modified slightly from Eq. (2.4)) is

$$\psi_0(\vec{r}, t) = \frac{\phi_0(\vec{r}, t)}{1 + \phi_0(\vec{r}, t)},$$

$$\phi_0(\vec{r}, t) = e^{t(1+\nabla^2)} \left[\frac{\psi(\vec{r}, 0)}{1 - \psi(\vec{r}, 0)} \right]. \tag{3.3}$$

The approximate solution in Eq. (3.3) reduces to that in Eq. (2.4) in the limit of small $\psi(\vec{r}, 0)$. However, in contrast to the earlier solution, Eq. (3.3) yields the exact solution in the homogeneous case $\psi(\vec{r}, 0) = \bar{\psi}(0)$, viz.,

$$\bar{\psi}_0(t) = \frac{e^t \bar{\psi}(0)}{1 - \bar{\psi}(0) + e^t \bar{\psi}(0)}. \tag{3.4}$$

We will use the approximate solution in Eq. (3.3) as the starting point of a perturbative expansion, which yields a hierarchy of linear equations. First, notice that the exact pde obeyed by the solution $\psi_0(\vec{r}, t)$ is

$$\partial_t \psi_0(\vec{r}, t) = \psi_0 - \psi_0^2 + \nabla^2 \psi_0 + \frac{2(\nabla\psi_0)^2}{1 - \psi_0}. \tag{3.5}$$

We decompose the exact solution of the Fisher equation as $\psi = \psi_0 + \theta_0$, where θ_0 is the correction to the singular-perturbation solution. Then, the pde obeyed by $\theta_0(\vec{r}, t)$ is

$$\partial_t \theta_0(\vec{r}, t) = (1 - 2\psi_0)\theta_0 - \theta_0^2 + \nabla^2 \theta_0 - \frac{2(\nabla\phi_0)^2}{(1 + \phi_0)^3}. \tag{3.6}$$

We assume that θ_0 is small, and break it up as $\theta_0 = \psi_1 + \theta_1$, where ψ_1 solves the linear part of Eq. (3.6):

$$\partial_t \psi_1(\vec{r}, t) = (1 - 2\psi_0)\psi_1 + \nabla^2 \psi_1 - \frac{2(\nabla\phi_0)^2}{(1+\phi_0)^3}. \tag{3.7}$$

The exact pde obeyed by $\theta_1(\vec{r}, t)$ is then

$$\partial_t \theta_1(\vec{r}, t) = [1 - 2(\psi_0 + \psi_1)]\theta_1 - \theta_1^2 + \nabla^2 \theta_1 - \psi_1^2, \tag{3.8}$$

which has the same general form as Eq. (3.6).

This process can be continued indefinitely. At the nth level, we decompose as $\theta_{n-1} = \psi_n + \theta_n$, where ψ_n solves the linear version of the pde obeyed by θ_{n-1}. The corresponding pde obeyed by θ_n is then

$$\partial_t \theta_n(\vec{r}, t) = \left(1 - 2\sum_{k=0}^{n} \psi_k\right)\theta_n - \theta_n^2 + \nabla^2\theta_n - \psi_n^2. \tag{3.9}$$

The approximate perturbative solution at the nth level of iteration is then obtained as

$$\psi(\vec{r}, t) \simeq \sum_{k=0}^{n} \psi_k(\vec{r}, t). \tag{3.10}$$

The general form of the pdes obeyed by ψ_k (for $k \geq 1$) is

$$\partial_t \psi_k(\vec{r}, t) = a(\vec{r}, t)\psi_k + \nabla^2 \psi_k + b(\vec{r}, t), \tag{3.11}$$

where $a(\vec{r}, t)$ and $b(\vec{r}, t)$ are functions of space and time. A formal solution of Eq. (3.11) reads (somewhat symbolically):

$$\psi_k = \left(\partial_t - \nabla^2 - a\right)^{-1} b. \tag{3.12}$$

It can be expanded in a Taylor-series in a. Denoting $R(\vec{x}, t)$ as the functional inverse of $(\partial_t - \nabla^2)$, such that $(\partial_t - \nabla^2)R(\vec{x}, t) = \delta(\vec{x})\delta(t)$, Eq. (3.12) can be written as

$$\psi_k(\vec{r}, t) = \int_0^t \mathrm{d}t' \int \mathrm{d}\vec{r}' R(\vec{r} - \vec{r}', t - t')b(\vec{r}', t')$$
$$+ \int_0^t \mathrm{d}t' \int \mathrm{d}\vec{r}' \int_0^{t'} \mathrm{d}t'' \int \mathrm{d}\vec{r}'' R(\vec{r} - \vec{r}', t - t')a(\vec{r}', t')R(\vec{r}' - \vec{r}'', t' - t'')b(\vec{r}'', t'') + \ldots$$
$$\tag{3.13}$$

Note that for $b(\vec{r}, t) = \delta(t)\,\phi(\vec{r}, 0)$ and $a = 1$, we recover the solution to the linear part of Eq. (3.2).

We will demonstrate shortly that this perturbative expansion converges very rapidly to the exact solution. However, we stress that our interest in such an expansion is more methodological than operational, i.e., the above procedure converts the problem of solution of the nonlinear Fisher equation to a hierarchy of linear equations. Of course, the same procedure would serve to improve any approximate solution – the singular-perturbation result is merely a convenient starting point.

3.2 Time-Dependent Ginzburg-Landau Equation

Before we present our numerical results, it is relevant to discuss the corresponding procedure for the scalar TDGL equation. (The generalization to the n-component case is relatively straightforward.) The corresponding nonlinear transformation is obtained by solving the TDGL-equation for constant initial conditions and reads

$$\psi(\vec{r}, t) = \frac{\phi(\vec{r}, t)}{\sqrt{1 + \phi(\vec{r}, t)^2}} \,, \tag{3.14}$$

where ϕ is the appropriate auxiliary field. In this case, we confine ourselves to the physically interesting case with $|\psi| < 1$. The pde satisfied by $\phi(\vec{r}, t)$ is [12]

$$\partial_t \phi(\vec{r}, t) = \phi + \nabla^2 \phi - \frac{3\phi(\nabla\phi)^2}{1 + \phi^2}. \tag{3.15}$$

As before, the singular-perturbation solution is obtained by neglecting the nonlinear term on the RHS of Eq. (3.15) as follows:

$$\psi_0(\vec{r}, t) = \frac{\phi_0(\vec{r}, t)}{\sqrt{1 + \phi_0(\vec{r}, t)^2}},$$

$$\phi_0(\vec{r}, t) = e^{t(1+\nabla^2)} \left[\frac{\psi(\vec{r}, 0)}{\sqrt{1 - \psi(\vec{r}, 0)^2}} \right]. \tag{3.16}$$

This solution constitutes an improvement over the solution in Eq. (2.8) as it is exact in the homogeneous case. The exact pde satisfied by ψ_0 is then

$$\partial_t \psi_0(\vec{r}, t) = \psi_0 - \psi_0^3 + \nabla^2 \psi_0 + \frac{3\psi_0(\nabla\psi_0)^2}{1 - \psi_0^2}. \tag{3.17}$$

We decompose the solution of the TDGL equation as $\psi = \psi_0 + \theta_0$, where the pde obeyed by $\theta_0(\vec{r}, t)$ is

$$\partial_t \theta_0(\vec{r}, t) = (1 - 3\psi_0^2)\theta_0 - 3\psi_0\theta_0^2 - \theta_0^3 + \nabla^2\theta_0 - \frac{3\psi_0(\nabla\psi_0)^2}{1 - \psi_0^2}. \tag{3.18}$$

As before, we designate the solution of the linear part of this equation as $\psi_1(\vec{r}, t)$. If we decompose the overall solution as $\theta_0 = \psi_1 + \theta_1$, the pde obeyed by $\theta_1(\vec{r}, t)$ is

$$\partial_t \theta_1(\vec{r}, t) = [1 - 3(\psi_0 + \psi_1)^2]\theta_1 - 3(\psi_0 + \psi_1)\theta_1^2 - \theta_1^3 + \nabla^2\theta_1 - (3\psi_0 + \psi_1)\psi_1^2. \tag{3.19}$$

Again, we can develop an infinite hierarchy of equations. The pde for $\theta_n(\vec{r}, t)$ at the nth level of this hierarchy is

$$\partial_t \theta_n(\vec{r}, t) = \left[1 - 3\left(\sum_{k=0}^{n} \psi_k\right)^2\right]\theta_n - 3\left(\sum_{k=0}^{n} \psi_k\right)\theta_n^2 - \theta_n^3 + \nabla^2\theta_n - \left(3\sum_{k=0}^{n-1} \psi_k + \psi_n\right)\psi_n^2. \tag{3.20}$$

Therefore, the problem of solution of the nonlinear TDGL equation is again reducible to the solution of an infinite hierarchy of linear equations for $\psi_k(\vec{r}, t)$. The approximate perturbative solution at the nth level is given by Eq. (3.10).

3.3 Numerical Results for the Fisher Equation

In this subsection, we will numerically examine the convergence properties of the hierarchy of linear equations presented above. For the sake of brevity, we confine ourselves to presenting numerical results for the Fisher equation in $d = 1, 2$. Similar results are obtained for the TDGL equation also.

Our numerical results for the Fisher equation, referred to as the "exact solution" subsequently, were obtained by implementing an Euler-discretized version of Eq. (2.1) (with an isotropic Laplacian) in $d = 1, 2$. In both cases, we used periodic boundary conditions. The discretization mesh sizes in $d = 1$ were $\Delta t = 0.001$ and $\Delta x = 0.1$ in time and space, respectively. The corresponding mesh sizes in $d = 2$ were $\Delta t = 0.001$ and $\Delta x = 0.2$. The lattice size was $N_1 = 40000$ in $d = 1$, and $N_2^2 = 1000^2$ in $d = 2$. The spatial coordinates are $x \in [-2000, 2000]$ in $d = 1$; and $x, y \in [-100, 100]$ in $d = 2$. Our perturbative solutions for ψ_0, ψ_1, ψ_2, etc. were also obtained numerically by solving the relevant linearized equations. The discretization meshes and lattice sizes for the perturbative solutions are identical to those described above.

Figure 1(a) shows the profile of a front arising from a seed initial condition ($\psi(x, 0) = 0.05\delta(x)$) for the $d = 1$ Fisher equation. The evolution gives two equivalent clines moving in opposite directions – we focus on the cline with $v > 0$. In Figure 1(a), we show the exact solution (solid line); the singular-perturbation or $n = 0$ solution (dashed line); the $n = 1$ solution (dotted line); and the $n = 2$ solution (dot-dashed line). The $n = 3$ perturbative solution (dot-dot-dashed line) is already numerically indistinguishable from the exact solution on the scale of the figure – we will quantify the error shortly. We have numerically confirmed that the perturbation series in Eq. (3.10) is strongly convergent, and the inclusion of higher-order terms ($n > 3$) does not change the solution appreciably.

Let us next examine the time-dependence of the front velocity. Recall that the $n = 0$ solution did not exhibit the correct approach to the asymptotic velocity $v = 2$. Figure 1(b) plots $v(t)$ vs. t^{-1} for the solutions depicted in Figure 1(a). Again, we see that the $n = 3$ result is almost coincident with the exact result.

Figures 2(a)-(b) study the evolution of the $d = 1$ Fisher equation from a random initial condition, consisting of 10 randomly-distributed seeds of random height (between 0 and 0.1). In Figures 2(a)-(b), we focus on the collision and merger of two fronts, showing the exact solution, and the solutions for $n = 0, 1, 3$. As in Figure 1(a), the $n = 3$ solution is numerically indistinguishable from the exact solution.

To quantify the error involved in our approximations, we compute the "distance" between the exact solution $\psi_e(x, t)$ and an approximate solution $\psi_a(x, t)$ as follows:

$$D(t) = \frac{1}{L} \int\limits_{-L/2}^{L/2} dx \, |\psi_e(x, t) - \psi_a(x, t)|, \tag{3.21}$$

where L is the lattice length. Figure 2(c) plots $D(t)$ vs. t on a semi-logarithmic scale for the different solutions depicted in Figures 2(a)-(b). We obtain $D(t)$ by averaging over 25 independent initial conditions constructed as the random superposition of seeds, Gaussians, sine-cosine functions, etc. The maximum error for the $n = 3$ solution is three orders of magnitude smaller than that for the $n = 0$ (singular-perturbation) solution. This quantifies the rapid convergence of our perturbative hierarchy. Of course, the error asymptotically approaches zero for all solutions as $\psi \to \psi^* = 1$ everywhere.

Next, we consider results for the $d = 2$ Fisher equation. Figure 3(a) shows an evolution snapshot obtained from a seed initial condition $\psi(x, y, 0) = 0.05\delta(x)\delta(y)$. The dark circular region refers to the exact solution, and denotes points where $\psi \geq 0.5$. The solid line refers to the front position for the $n = 0$ solution, and is defined by points where $\psi = 0.5$. Figure 3(b) shows the corresponding variation of the order parameter along a horizontal cross-section of the lattice. As in the $d = 1$ case, the singular-perturbation

front is appreciably sharper than the exact front. For clarity, we do not show the higher-order perturbation results – as before, the $n = 3$ result is indistinguishable from the exact solution. We focus on the front position so as to clarify the convergence of the perturbative solution. Figure 3(c) plots the front velocity $v(t)$ vs. t^{-1} for the solutions depicted in Figure 3(b).

Finally, Figures 4(a)-(b) study the evolution from a random initial condition for the $d = 2$ Fisher equation. The initial condition consists of 25 randomly-distributed seeds with amplitudes between 0 and 0.1. Figure 4(a) shows an evolution snapshot at $t = 12$. (For clarity, we only show a 500^2 corner of the 1000^2 lattice.) The coding is the same as that for Figure 3(a). Figure 4(b) shows the variation of the order parameter along a horizontal cross-section of the snapshot shown partially in Figure 4(a). We present results for the exact solution, and approximate solutions with $n = 0, 1, 3$. The approximation error is quantified in Figure 4(c), where we plot $D(t)$ vs. t on a semi-logarithmic scale. The error is obtained as the $d = 2$ generalization of the quantity defined in Eq. (3.21). As in the $d = 1$ case, the error was obtained as an average over 25 independent initial conditions of different types.

4 Summary and Discussion

Let us conclude this paper with a summary and discussion of the results presented here. We have studied two important examples of reaction-diffusion systems, viz., the Fisher equation and the time-dependent Ginzburg-Landau (TDGL) equation. We are interested in the linearization of these and other reaction-diffusion equations, i.e., conversion of the nonlinear problem to a linear problem. In both cases, we find that the singular-perturbation solution is a good starting point for a perturbative expansion. This expansion transforms the problem of solution of the nonlinear partial differential equation to the solution of a hierarchy of linear partial differential equations. Our numerical studies demonstrate that this hierarchy rapidly converges to the exact solution of the relevant equation. However, we should stress that our primary interests in this paper are methodological rather than operational.

The techniques developed here are of general applicability to a wide range of reaction-diffusion equations. Of course, any approximate solution to the initial-value problem for a given equation is a good starting point for a perturbative expansion. However, we find that the singular-perturbation solution appears to be particularly convenient in that it yields an extremely accurate solution within a few steps of the perturbation expansion.

Acknowledgements

References

[1] M.J. Ablowitz and H. Segur, *Solitons and the Inverse Scattering Transform*, SIAM Studies in Applied Mathematics, SIAM Press, Philadelphia (1981).

[2] S. Puri, Int. J. Mod. Phys. B **4**, 1483 (1990).

[3] H. Meinhardt, *Models for Biological Pattern Formation*, Academic, London (1982).

[4] Y. Kuramoto, *Chemical Oscillations, Waves and Turbulence*, Springer-Verlag, Berlin (1984).

[5] W. van Saarloos, in *Spatiotemporal Patterns in Nonequilibrium Systems*, ed. P.E. Cladis and P. Palffy-Muhoray, Addison-Wesley, Reading, MA (1994).

[6] M.C. Cross and P.C. Hohenberg, Rev. Mod. Phys. **65**, 851 (1993).

[7] E. Hopf, Commun. Pure Appl. Math. **3**, 201 (1950); J.D. Cole, Quart. Appl. Math. **9**, 225 (1951).

[8] J. Burgers, *The Nonlinear Diffusion Equation*, Dordrecht, Reidel (1974).

[9] R.A. Fisher, Ann. Eugenics **7**, 355 (1937).

[10] A.N. Kolmogorov, I.G. Petrovskii and N.S. Piscounov, Bull. Univ. Moscow Ser. Int. Sec. A **1**, 1 (1937).

[11] P.C. Hohenberg and B.I. Halperin, Rev. Mod. Phys. **49**, 435 (1977).

[12] A.J. Bray, Adv. in Physics **43**, 357 (1994).

[13] D.G. Aronson and H.F. Weinberger, in *Partial Differential Equations and Related Topics*, ed. J.A. Goldstein, Springer, Berlin, pp. 5-49 (1975); see also Adv. Math. **30**, 33 (1978).

[14] J.S. Langer and H. Müller-Krumbhaar, Phys. Rev. A **27**, 499 (1983); G. Dee and J.S. Langer, Phys. Rev. Lett. **50**, 6 (1983); W. van Saarloos, Phys. Rev. Lett. **58**, 24 (1987); W. van Saarloos, Phys. Rev. A **37**, 1 (1988).

[15] G.C. Paquette, L.-Y. Chen, N. Goldenfeld and Y. Oono, Phys. Rev. Lett. **72**, 76 (1994); G.C. Paquette and Y. Oono, Phys. Rev. E **49**, 2368 (1994).

[16] M.J. Ablowitz and F. Zeppetella, Bull. Math. Biol. **41**, 835 (1979); see also B.-Y. Guo and Z.-X. Chen, J. Phys. A **24**, 645 (1991).

[17] S. Puri, K.R. Elder and R.C. Desai, Phys. Lett. A **142**, 357 (1989); S. Puri, Phys. Rev. A **43**, 7031 (1991).

[18] M. Suzuki, Prog. Theor. Phys. **56**, 477 (1976).

[19] K. Kawasaki, M.C. Yalabik and J.D. Gunton, Phys. Rev. A **17**, 455 (1978).

[20] M. Bramson, Mem. Am. Math. Soc. **285**, 1 (1983).

[21] S. Puri and A.J. Bray, J. Phys. A **27**, 453 (1994).

[22] S. Puri and C. Roland, Phys. Lett. A **151**, 500 (1990).

[23] A.J. Bray and S. Puri, Phys. Rev. Lett. **67**, 2670 (1991).
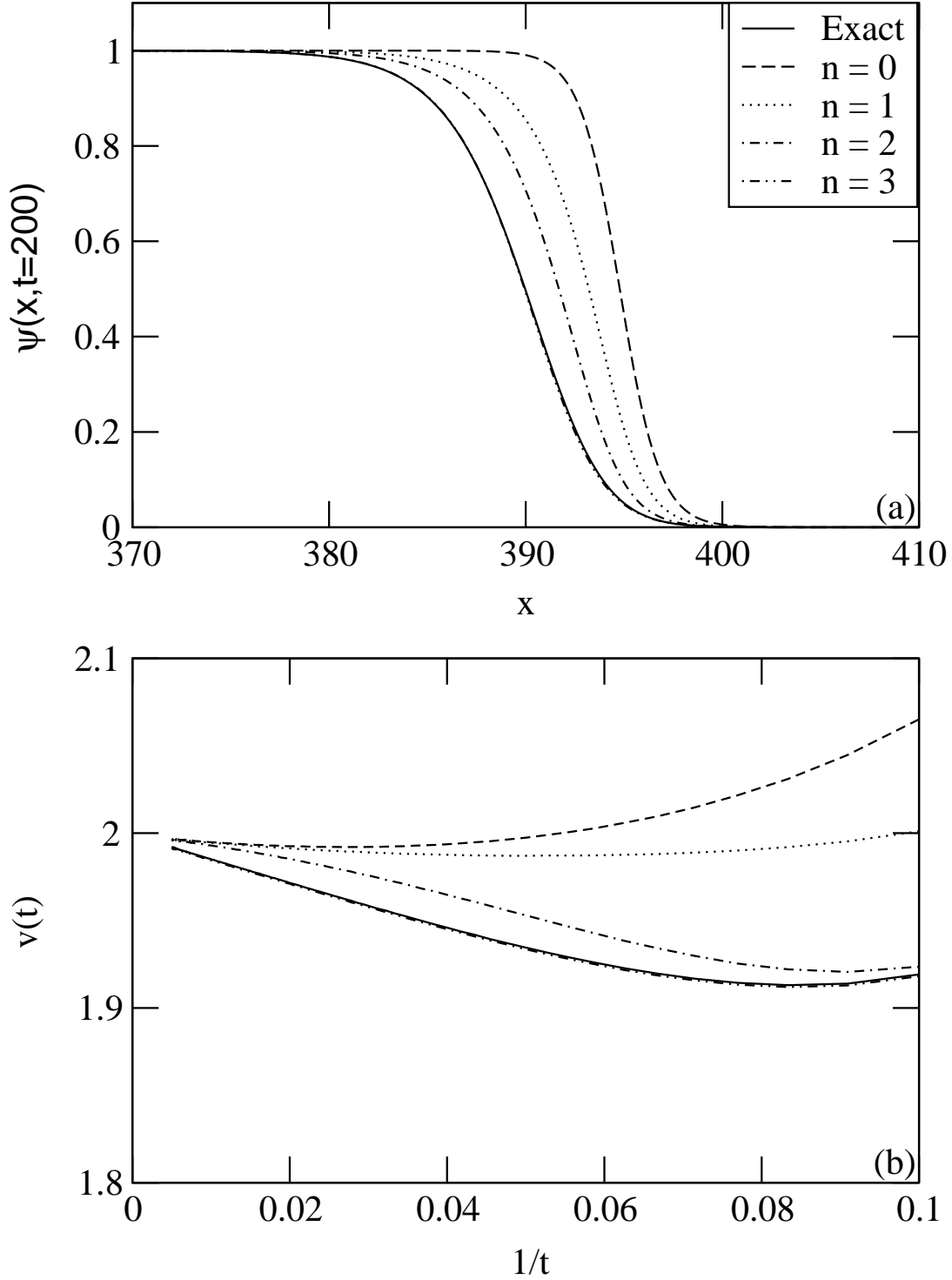
[24] S. Puri, Phys. Lett. A **164**, 211 (1992).

Figure 1: (a) Evolution snapshot of the $d = 1$ Fisher equation for a seed initial condition $\psi(x, 0) = 0.05\delta(x)$. We plot the order parameter $\psi(x, t = 200)$ vs. x for the front moving with velocity $v > 0$. Details of our simulation are provided in the text. We present results for the exact solution (solid line); the singular-perturbation or $n = 0$ solution (dashed line); the $n = 1$ solution (dotted line); the $n = 2$ solution (dot-dashed line); and the $n = 3$ solution (dot-dot-dashed line). (b) Plot of front velocity $v(t)$ vs. t^{-1} for the solutions depicted in (a). The line-type usage is the same as that in (a).
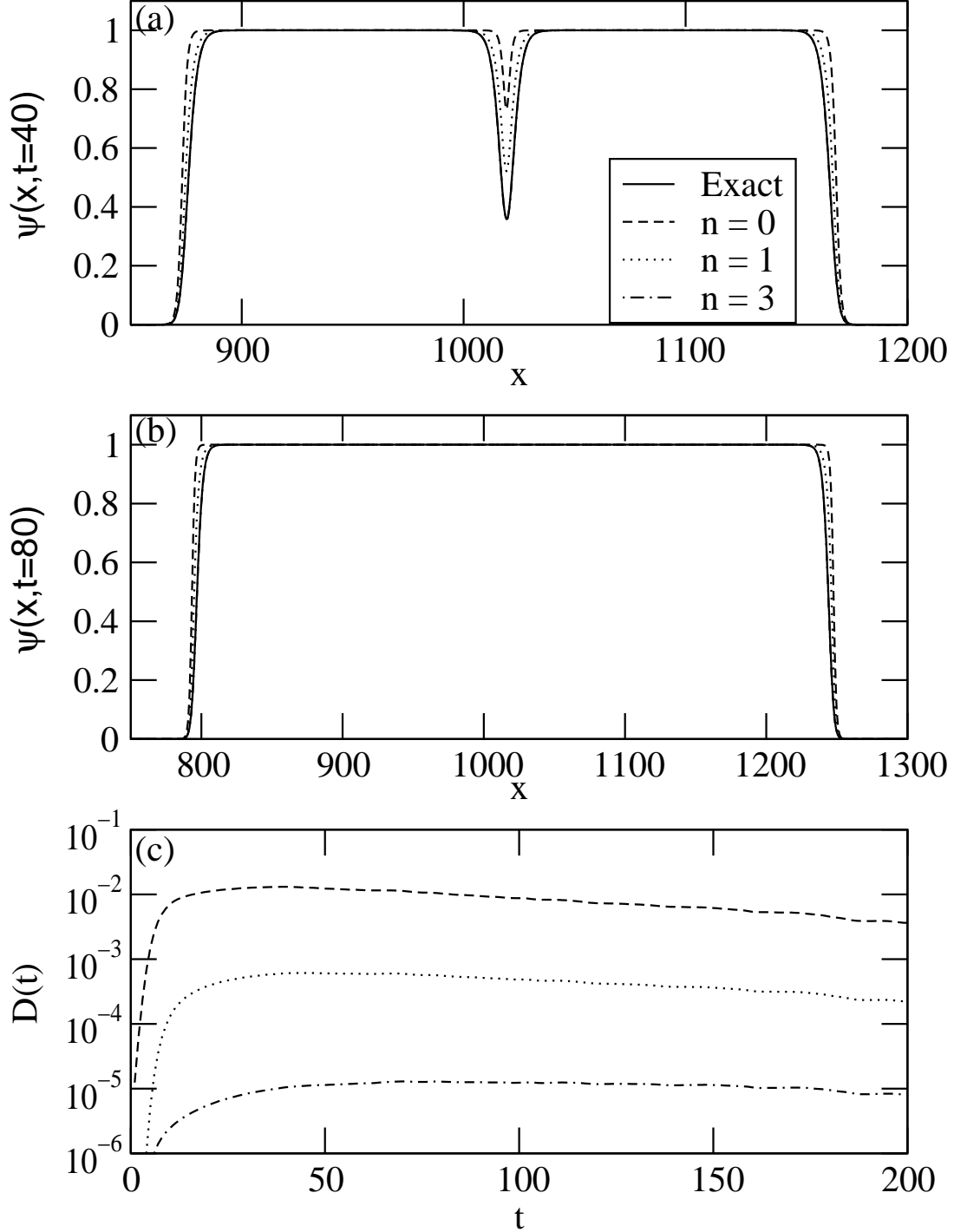
Figure 2: (a) Evolution snapshot of the $d = 1$ Fisher equation for a random initial condition, consisting of 10 randomly-distributed seeds of amplitude between 0 and 0.1. We plot the order parameter $\psi(x,t)$ vs. x at $t = 40$, focusing on a front-front collision. The results shown are analogous to those in Figure 1(a), except we do not show the case $n = 2$. (b) Analogous to (a), but at the later time $t = 80$. (c) Plot of $D(t)$ vs. t on a semi-logarithmic scale, where $D(t)$ is the "distance" (defined in Eq. (3.21)) between the exact solution and an approximate solution. The error $D(t)$ is obtained as an average over 25 independent initial conditions of various types. We show results for the approximate solutions with $n = 0, 1, 3$, using the same line-types as in (a)-(b).
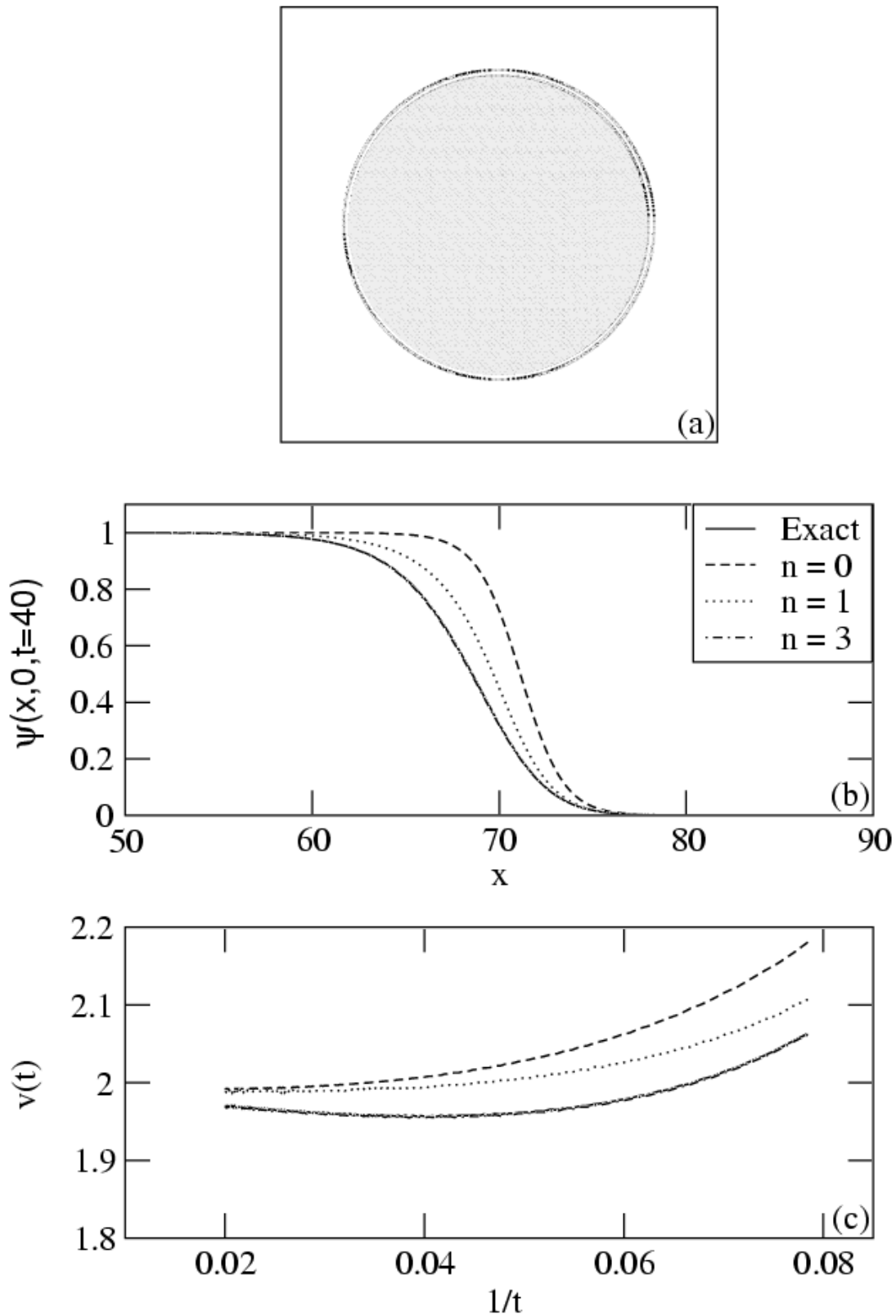
Figure 3: (a) Evolution snapshot of the $d = 2$ Fisher equation from a seed initial condition $\psi(x, y, 0) = 0.05\delta(x)\delta(y)$. The dark region corresponds to the exact solution at $t = 40$, and denotes points where $\psi \geq 0.5$. The solid line refers to the singular-perturbation ($n = 0$) solution at $t = 40$, and denotes points where $\psi = 0.5$. (b) Variation of the order parameter along a horizontal cross-section for the evolution depicted in (a). We plot $\psi(x, y, t = 40)$ vs. x for $y = 0$, and focus on the front solution. The results presented are analogous to those in Figure 2(a). (c) Plot of front velocity $v(t)$ vs. t^{-1} for the solutions depicted in (b).
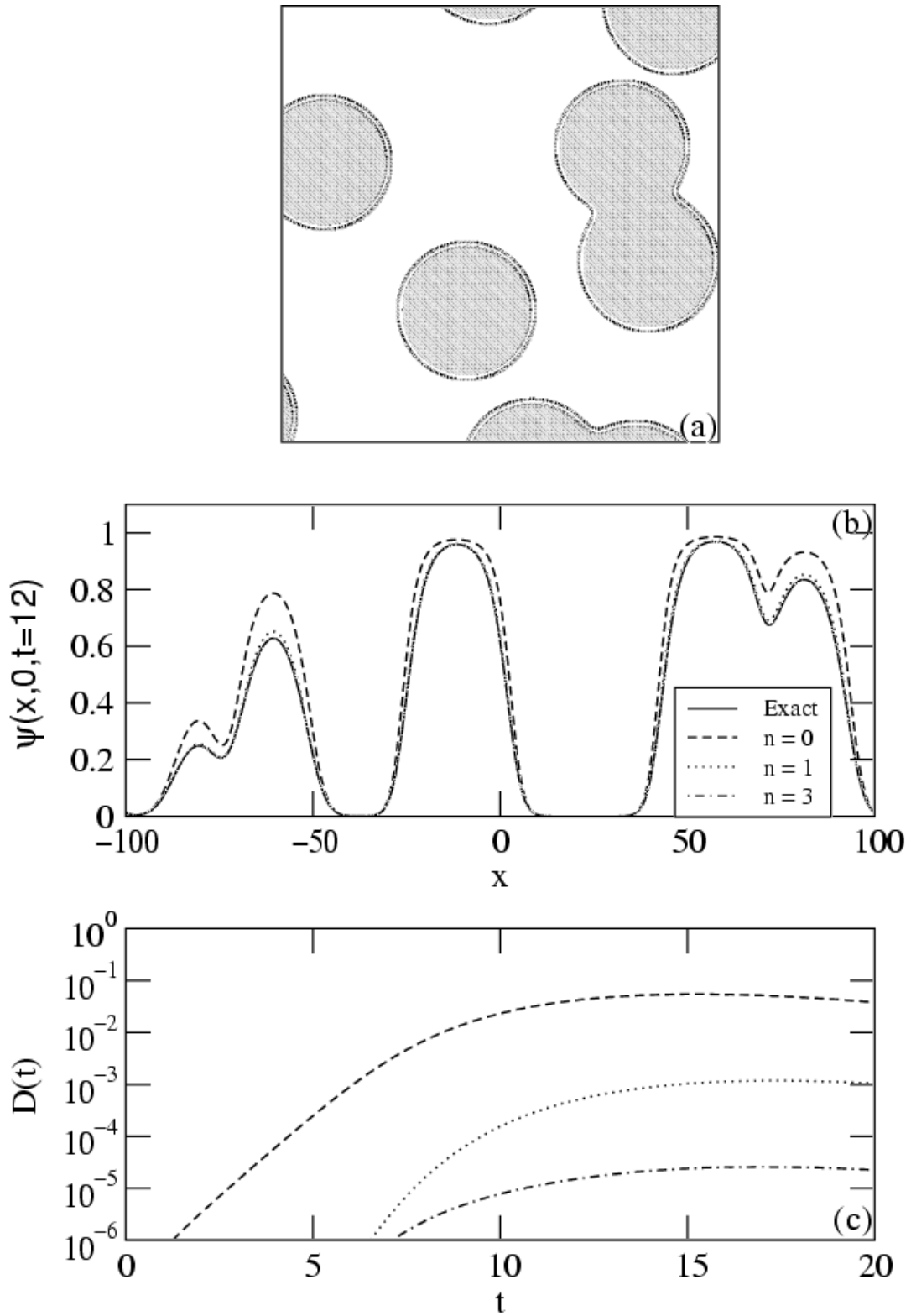
Figure 4: (a) Evolution snapshot of the $d = 2$ Fisher equation from a random initial condition, consisting of 25 randomly-distributed seeds with amplitude between 0 and 0.1. The dark regions denote the exact solution at $t = 12$, and the solid line denotes the corresponding singular-perturbation solution. For clarity, we only show a 500^2 corner of the 1000^2 lattice. (b) Variation of the order parameter along a horizontal cross-section of the snapshot partly shown in (a). We plot $\psi(x, y = 0, t = 12)$ vs. x for the entire range of x-values. The line-type usage is the same as earlier. (c) Analogous to Figure 2(c), but for the $d = 2$ Fisher equation.